CHEMICAL ENGINEERING TRANSACTIONS

VOL. 122, 2025

A publication of AIDIC

The Italian Association of Chemical Engineering
Online at www.cetjournal.it

Guest Editors: Jeng Shiun Lim, Bohong Wang, Guo Ren Mong, Petar S. Varbanov

ISBN 979-12-81206-23-6; **ISSN** 2283-9216

DOI: 10.3303/CET25122068

Comparison of Boron and Carbon-doping on Molybdenum Substrate via CVD for Hydrogen Evolution Reaction (HER)

Dayang Amirah Nabihah Awang Tambun[a], Muhammad Aniq Syazni Mohammad Haniff[b], Ibrahim Yakub[a], Mohammad Omar Abdullah[a], Harunal Rejan Ramji[a,*]

[a]Hydrogen Production, Techno-economy and Sustainability (HPTeS) Group, Faculty of Engineering, Universiti Malaysia Sarawak (UNIMAS), Kota Samarahan, Malaysia
[b]Institute of Microengineering & Nanoelectronics (IMEN), Level 4, Research Complex, Universiti Kebangsaan Malaysia (UKM), 43600, Bangi, Selangor, Malaysia
rhrejan@unimas.my

In this study, boron (B-Mo) and carbon (C-Mo) were synthesized via chemical vapor deposition (CVD) on bulk molybdenum substrate to investigate the comparative effects of dopant species on material structure and HER performance in acidic media. Structural characterization revealed that C-Mo exhibited amorphous carbon layers with partially disordered graphitic domains, whereas B-Mo formed uniform boron-rich layers with increased surface roughness and porosity. Electrochemical testing in 0.5 M H_2SO_4 showed that B-Mo achieved a lower overpotential of 439 mV at 10 mA/cm² compared to 456 mV for C-Mo, indicating superior HER activity for boron doping. Tafel slope analysis supported this trend, with B-Mo exhibiting a slope of 296 mV $\cdot$dec^{-1} and 282 mV$\cdot$dec^{-1} for C-Mo, suggesting almost equivalent kinetics. The relationship between dopant type, surface morphology, and electrochemical behavior was systematically explored to identify the optimal dopant for HER enhancement. This work provides important insights into the rational design of doped molybdenum electrocatalysts and advances the development of cost-effective materials for sustainable hydrogen production.

1. Introduction

Hydrogen production via water electrolysis is a promising clean energy solution. It involves two half-reactions: the hydrogen evolution reaction (HER) at the cathode and the oxygen evolution reaction (OER) at the anode (Soriano et al., 2023). HER entails the reduction of protons (in acidic media) or water molecules (in alkaline media) to generate hydrogen gas (H_2) (Wei et al., 2007). The HER proceeds through three main steps, which are Volmer step (formation of adsorbed hydrogen (H_{ads}), Heyrovsky step (electrochemical combination of a proton with H_{ads} to form H_2), and Tafel step (chemical recombination of two H_{ads} species to release H_2 gas) (Ramji et al., 2025). Introducing metalloids like boron into the lattice or surface of molybdenum offers a viable pathway to modulate the electronic configuration and local chemical environment of active sites (Saini et al., 2023). Boron doping into Mo has been shown to effectively alter the binding energies of key intermediates, thereby improving reactivity, selectivity, and long-term durability in electrochemical reactions such as the hydrogen evolution reaction (HER) (Wang et al., 2017). On the other hand, carbon doping contributes significantly to enhanced conductivity and defect generation, which facilitates charge transfer and intermediate adsorption (Kou et al., 2020). Combining both dopants or systematically comparing their effects may offer synergistic advantages, where boron's electron-deficient nature and carbon's electron-donating properties jointly influence the local electron density and hydrogen adsorption energy (Shiva Kumar and Himabindu, 2020). These modifications enable fine control over the Volmer, Heyrovsky, and Tafel steps of HER(Shinagawa et al., 2015). SEM-EDX-Mapping, along with electrochemical characterization, has provided insights into how the individual doping of boron and carbon tunes surface reactivity at the microstructure.

Recent studies show that dopant engineering improves molybdenum-based catalysts for water splitting (Hua et al., 2020). However, direct comparisons of boron and carbon doping effects on molybdenum under identical conditions are still limited. This study compares the impact of boron and carbon doping on the HER activity of

Paper Received: 14 June 2025; Revised: 3 August 2025; Accepted: 27 September 2025
Please cite this article as: Awang Tambun D.A.N., Mohammad Haniff M.A.S., Yakub I., Abdullah M.O., Ramji H.R., 2025, Comparison of Boron and Carbon-doping on Molybdenum Substrate via CVD for Hydrogen Evolution Reaction (HER), Chemical Engineering Transactions, 122, 403-408 DOI:10.3303/CET25122068

molybdenum sheet. Doping was done separately via CVD, and the samples were characterized for surface morphology, elemental distribution, and electrochemical behavior. This work aims to determine the optimal dopant (boron or carbon) for enhancing HER activity and to evaluate how each dopant influences the charge transfer characteristics and hydrogen adsorption behavior. The insights gained from this study are expected to contribute to the rational design of next-generation, non-noble metal-based electrocatalysts for sustainable hydrogen production.

2. Methodology

2.1 Materials Preparation

Molybdenum (Mo) sheet (99.9 % purity; dimensions: 150 mm × 300 mm × 50 mm) was used as the substrate. The Mo sheet pieces were dissolved in ethanol for 5 min, followed by rinsing in distilled water for 5 min, and finally in isopropanol (IPA) for 5 min to remove surface contaminants. The cleaned Mo sheet was placed on a porcelain boat and inserted into a horizontal quartz tube (inner diameter: 25.4 mm; length: 40 cm) at room temperature.

2.1.1 Carbon Doping Process (C-Mo)

The quartz tube was sealed and purged with an Ar/H_2 gas mixture for 30 min at atmospheric pressure to eliminate residual air. While maintaining the Ar/H_2 flow, the system was heated to 700 °C at a ramp rate of 11.25 °C/min. The Mo sheet was annealed at 700 °C for 60 min under the Ar/H_2 environment to enhance surface smoothness, reduce native oxides, and promote grain growth. Following the annealing step, a carbon source was introduced by heating sucrose powder (Kumar et al., 2018) upstream to thermally decompose it into carbon and water vapor according to the Eq(1).

$$C_{12}H_{22}O_{11}(s) \underset{\Delta}{\rightarrow} 12C(g) + 11H_2O(l) \tag{1}$$

The resulting carbon atoms in the gas phase interacted with the Mo surface, leading to their adsorption and incorporation in Eq(2):

$$C(g) + Mo(s) \rightarrow C - Mo(s) \tag{2}$$

The generated carbon atoms were carried downstream by the Ar/H_2 flow and deposited onto the Mo surface, is represented in Eq(2). This in-situ decomposition synergistically enabled a uniform supply of reactive carbon species, facilitating carbon incorporation onto the Mo sheet at 700 °C. The carbon growth was maintained at 700 °C for 60 min with a constant total gas flow rate of 150 sccm. Upon completion of the growth process, the heating of the sucrose powder was stopped, effectively ceasing the generation of carbon vapor. The system was then allowed to cool to room temperature under continuous Ar/H_2 flow to prevent oxidation and preserve the carbon-doped surface.

2.1.2 Boron Doping Process (B-Mo)

A separate porcelain crucible containing a solid pellet mixture of sodium borohydride ($NaBH_4$) and iodine (I_2) in a 2:1 molar ratio for the formation of diborane gas (Gigante, 2020) was placed upstream from the sample zone. Upon heating, the components reacted according to Eq(3):

$$2NaBH_4(s) + I_2(s) \underset{\Delta}{\rightarrow} B_2H_6(\mathrm{g}) + 2NaI(s) + H_2(g) \tag{3}$$

Followed by thermal decomposition of diborane to supply elemental boron (Mazaheri et al., 2021) in Eq(4):

$$B_2H_6(g) \overset{\Delta}{\rightarrow} 2\mathrm{B}(\mathrm{s}) + 3H_2(g) \tag{4}$$

The atomic boron produced was carried by the Ar/H_2 stream and deposited onto the Mo surface through adsorption and incorporation processes, which represented in Eq(5):

$$B(g) + Mo(s) \rightarrow B - Mo\ (s) \tag{5}$$

The pellet form ensured a gradual and localized release of volatile boron species during the doping process. This mixture serves as the boron source and decomposes to release volatile boron-containing species during heating. After sealing the quartz tube, it was purged with an Ar/H_2 (95:5) gas mixture at a total flow rate of 150 sccm for 30 min to expel residual air. Under continuous Ar/H_2 flow, the furnace temperature was increased to 700 °C. Once the target temperature was reached, the $2NaBH_4/I_2$ mixture was gradually heated by moving the upstream crucible into the heating zone or by applying a separate heating mantle to initiate sublimation and reaction. The boron doping process was maintained for 60 min at 700 °C at a ramp rate of 11.25 °C/min, during which boron species were carried downstream by the Ar/H_2 flow to react with the Mo substrate. After 60 min of reaction, the heating was turned off, and the system was allowed to cool naturally to room temperature under continuous Ar/H_2 flow. The resulting boron-doped Mo samples were collected and stored in an inert atmosphere until further use or characterization according to Eq(5). The use of systematic doping (boron and carbon) on molybdenum foils via identical CVD conditions and subsequent electrochemical testing allows for a controlled comparison of their individual effects on HER performance. This approach ensures that any observed differences in catalytic activity can be attributed primarily to the dopant type rather than other variables.

2.2 Instrumentations for structural and compositional characterization

The structural and compositional properties of the materials were analyzed using several techniques. Optical microscopy (Meiji Techno MT4000) was employed for surface morphology observation, while scanning electron microscopy (SEM, Hitachi S-3400N) with energy-dispersive X-ray spectroscopy (EDX, Bruker XFlash, Germany) was used to obtain high-resolution images and elemental composition of the samples.

2.3 Electrochemical study

A three-electrode system was employed to evaluate the electrochemical performance of the electrocatalysts. The reference electrode was an Ag/AgCl electrode, and a platinum wire served as the counter electrode. Bare molybdenum (Mo), carbon-doped Mo (C–Mo), and boron-doped Mo (B–Mo) samples synthesized at 700 °C were used as working electrodes. Linear Sweep Voltammetry (LSV) measurements were performed using a ZIVE Smart Manager potentiostat/ galvanostat system. The experiments were conducted in 0.5 M H_2SO_4 electrolyte at room temperature. All measurements were carried out within a potential window suitable for observing the hydrogen evolution reaction (HER), using a scan rate of 10 mV/s.

3. Results and Discussion

3.1 Morphology and Structural of Mo, C-Mo, and B-Mo

The optical microscopy images in Figure 1a-c, provide a macroscopic view of the samples, revealing distinct visual differences among bare Mo, B-Mo, and C-Mo, all treated at 700 °C. The bare Mo (Figure 1a) surface appears smooth and reflective with minimal surface features. Upon doping, the B–Mo (Figure 1c) sample shows a moderately darkened appearance with visible textural changes, while the C–Mo (Figure 1b) sample exhibits the darkest surface among the three, suggesting a thicker or denser carbon deposition. The progressive darkening trend (bare Mo < B–Mo < C–Mo) generally reflects increased surface modification, but the B–Mo structure appears to balance surface roughness. These initial observations were further supported by SEM analysis, which revealed enhanced surface porosity in the B–Mo sample, contributing to its catalytic performance.

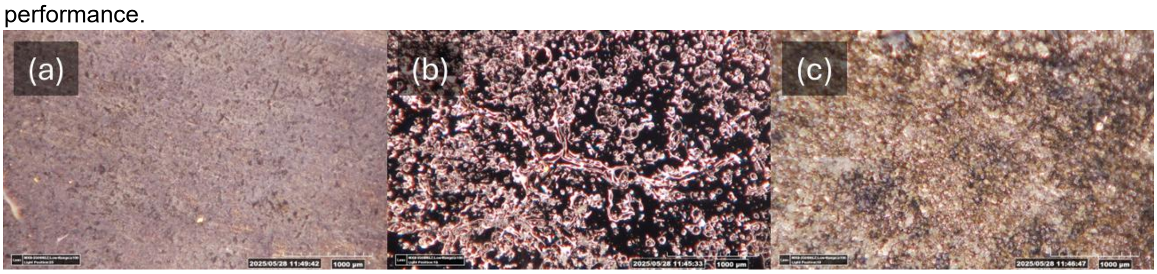

Figure 1: Optical microscope Images of (a) Bare Mo Foil, (b) C-Mo, (c) B-Mo

SEM analysis (Figure 2) provides detailed insights into the microstructural variations among the samples, further validating the textural differences observed in optical microscopy. As shown in Figure 2a, the surface of bare Mo is relatively smooth with minimal porosity, indicative of a pristine metallic substrate. In contrast, C–Mo sample (Figure 2b) exhibits a bulky and dense surface morphology, suggesting the formation of thick carbonaceous layers with limited porosity. This dense coverage may hinder the accessibility of active sites and restrict reactant diffusion, potentially reducing electrocatalytic efficiency. Interestingly, B–Mo sample (Figure 2c) displays a markedly more porous microstructure, with fine, interconnected features distributed across the surface. This porosity is favorable for HER activity, as it increases the electrochemically active surface area and facilitates better interaction between the catalyst and electrolyte. These findings clearly demonstrate that the nature of the dopant significantly influences the surface architecture of Mo-based catalysts. While C–Mo shows extensive surface modification, its bulky structure may not be ideal for catalysis. Conversely, B–Mo achieves a desirable balance of porosity and surface roughness, which correlates with its superior HER performance.

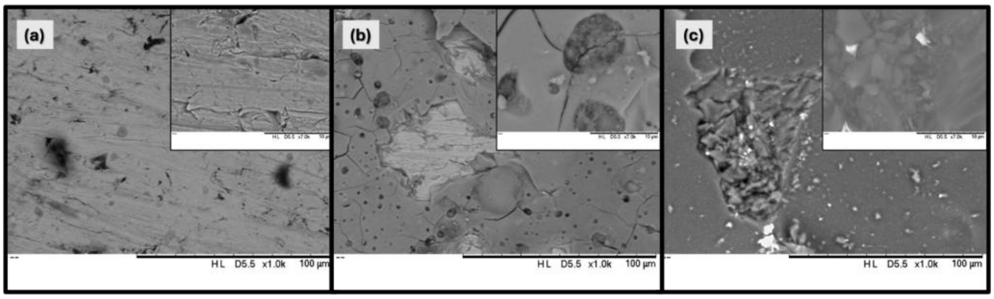

Figure 2: SEM images of a (a) Bare Mo, (b) C-Mo, and (c) B-Mo

EDX with elemental mapping (Figure 3) confirms that all samples are primarily composed of Mo as the dominant element. In the C–Mo, a significant carbon signal is detected, confirming successful carbon incorporation during the doping process. In contrast, B–Mo exhibits traces of iodine (I), sulfur (S), and oxygen (O). distributed across the surface, along with a minor iodine signal, which likely originates from the use of iodine as a facilitating agent during the boron doping reaction. This suggests effective interaction or substitution of boron within or on the Mo surface, even at trace levels. Additionally, B–Mo samples show minor levels of sulfur (S) and oxygen (O). These elements are likely due to environmental exposure, surface oxidation, or residual impurities, and are not part of the intended material composition. Oxygen is especially associated with the rapid formation of a native oxide layer on Mo upon exposure to air, while sulfur may originate from contamination during processing or storage. The elemental mapping at 700 °C demonstrates a relatively uniform distribution of the dopants across the Mo surface in both C–Mo (Figure 3a) and B–Mo (Figure 3b) samples. In C–Mo, carbon is seen coating the surface densely, while in B–Mo, the elemental maps confirm the presence of dispersed boron and iodine, despite their low concentration.

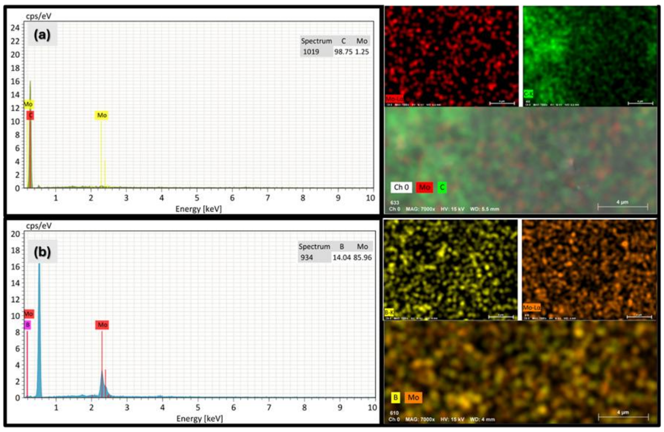

Figure 3: EDX-mapping of a (a) C-Mo and (b) B-Mo

3.2 Electrochemical Performance of Mo, C-Mo, and B-Mo

Figure 4a shows the polarization curves of bare Mo, C–Mo, and B–Mo synthesized at 700 °C in 0.5 M H_2SO_4. Linear sweep voltammetry (LSV) was used to evaluate their HER activity. B–Mo exhibits the lowest overpotential ($\eta_{10} \approx$ 439 mV), followed by C–Mo ($\eta_{10} \approx$ 456 mV) and bare Mo ($\eta_{10} \approx$ 466 mV), indicating the beneficial effect of boron doping. While C–Mo delivers higher currents at potentials beyond −0.7 V, B–Mo shows superior kinetics at practical current densities. The enhancement in B–Mo is attributed to the synergistic effect of boron incorporation, which modulates the Mo surface electronic structure, introduces active sites, and facilitates hydrogen adsorption and desorption steps more efficiently than carbon (Guo et al., 2020). Interestingly, the C–Mo, despite exhibiting darker features in structural imaging (suggesting denser or more graphitic carbon), does not surpass the HER performance of B–Mo. This indicates that while carbon may contribute to conductivity and surface roughness, boron doping has more significant impact on intrinsic catalytic activity (Shiva Kumar and Himabindu, 2020). Full comparison with other Mo-based HER catalysts is summarized in Table 1. Notably, this work focuses on self-supporting bulk electrodes, unlike many prior studies which used drop-cast catalysts on glassy carbon electrodes (GCEs), such as MoC, and MoO. This distinction eliminates the influence of external binders or substrates, allowing for a more intrinsic assessment of catalytic activity. This distinction eliminates the influence of external binders or substrates, allowing for a more intrinsic assessment of catalytic activity. Carbon and boron doping significantly reduced the overpotential to pristine Mo, highlighting enhanced HER activity. Based on Figure 4b, at low current density region (0–10 mA), Mo (Bulk) exhibits the highest Tafel slope of 303 mV·dec^{-1}, indicating sluggish HER kinetics likely governed by the Volmer step (proton adsorption) as the rate-determining step (Ramji et al., 2024). Upon carbon and boron doping, the Tafel slopes decrease to 282 mV·dec^{-1} for C-Mo (Bulk) and 296 mV·dec^{-1} for B-Mo (Bulk). This suggests improved proton transfer and surface conductivity. C-Mo shows a greater Tafel slope reduction than bare Mo, indicating a stronger effect of carbon doping on the initial adsorption process. At higher current densities (10–100 mA) in Figure 4c, the Tafel slopes of Mo and C-Mo remain close, at 251 mV·dec^{-1} and 252 mV·dec^{-1}, respectively, showing that carbon doping maintains comparable HER kinetics even under more demanding conditions. In contrast, B-Mo exhibits a higher slope of 297 mV·dec^{-1}, suggesting some limitation in H_2 recombination or mass transport resistance, possibly due to surface restructuring or partial saturation effects. However, the performance is still within a comparable range to bare Mo, indicating that boron doping does not severely hinder HER activity at higher currents.

Overall, both dopants, carbon and boron, contribute to modest improvements in HER kinetics relative to undoped Mo. The lower overpotential suggests that B-Mo requires less energy to drive the same current, pointing to enhanced HER kinetics likely due to favorable surface modifications induced by boron doping. Additionally, the Tafel slope also showed consistent improvement. The improvements observed here demonstrate the effectiveness of a simpler and more scalable thermal doping process using CVD. These results confirm that heteroatom doping can tune the electronic structure of Mo and enhance HER performance. This study provides valuable insight into the role of dopants in modulating HER activity and highlights a promising direction for future research, optimizing dopant type, concentration, and processing temperature to close the performance gap with more complex systems. Boron doping improves the HER activity of bulk Mo, particularly at lower overpotentials, by enhancing active site density and modifying the surface electronic structure. Meanwhile, carbon doping provides moderate improvements, balancing between conductivity and catalytic performance. The synergistic effects of boron and carbon species demonstrate their role in tuning the Mo surface and accelerating HER kinetics.

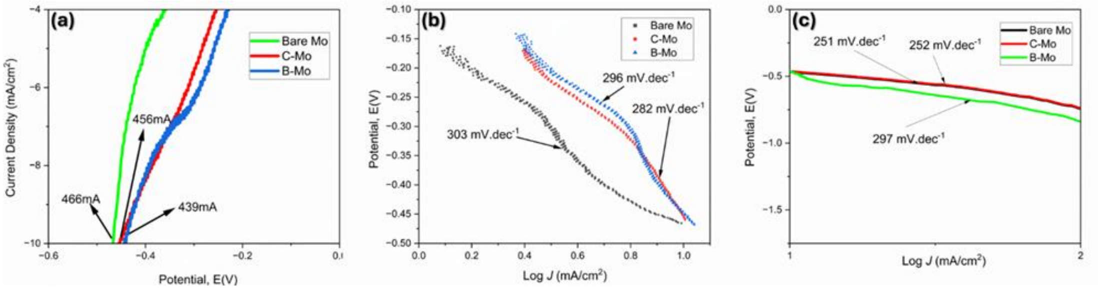

Figure 4: (a) LSV curve of Mo Foil, Tafel Plot of Mo Foil (b) 0~10 mA and (c) 10~100 mA

Table 1: Mo-based HER catalysts

d	Electrolyte	Overpotential mV	Tafel slope mV.dec^{-1}	Reference
Mo (Bulk)	0.5 H_2SO_4	466	251@10~100 mA 303@0~10mA	This work
C-Mo (Bulk)	0.5 H_2SO_4	456	252@10~100 mA 282@0~10mA	This work
B-Mo (Bulk)	0.5 H_2SO_4	439	297@10~100 296@0~10mA	This work
MoC (GCE)	0.5 H_2SO_4	450	165	Lin et al., 2020
MoB (GCE)	0.5 H_2SO_4	350	80	Ramji et al. 2023
MoO (GCE)	0.5 H_2SO_4	277	81.34	Sun et al. 2020

4. Conclusions

In conclusion, C-Mo and B-Mo sheet were successfully synthesized via CVD to improve HER performance. This study showed that B-Mo achieved a lower overpotential (439 mV) compared to C-Mo (456 mV) and bare Mo (466 mV), indicating better HER activity. Both boron and carbon doping enhanced the HER activity of molybdenum, with B-Mo showing the best performance. This confirms that boron is an effective dopant under acidic conditions, likely due to its electron-deficient nature, which improves H* adsorption. In contrast, carbon tends to act more effectively as a support or co-dopant in metal-containing systems. Boron doping also enhanced charge transfer and surface porosity more than carbon, as reflected by its lower overpotential. However, the Tafel slopes for both B-Mo (296 $mV \cdot dec^{-1}$) and C-Mo (282 $mV \cdot dec^{-1}$) suggest room for kinetic improvement. All electrochemical tests were performed in 0.5 M H_2SO_4, limiting the understanding of performance across different pH conditions. To improve future work, dopant levels should be varied and precisely measured to establish structure-activity relationships. Electrochemical stability testing and evaluations in multiple electrolytes are recommended to assess real-world applicability. Ultimately, DFT modelling and co-doping strategies may offer further insight and improve HER kinetics.

Acknowledgments

This work was supported by UNIMAS VC High Impact Research Grant no. UNI/F02/VC-HIRG-2/86090/2023.

References

Gigante, A., 2020, Archive ouverte UNIGE Novel and Scalable Synthesis of BnHxz-Boron Clusters as Solid-State Electrolytes for Sodium Batteries and their Detailed Study for Hydrogen Storage Applications, Doctoral Thesis, University of Geneva, Geneva, Switzerland.

Guo, Y., Yao, Z., Zhan, S., Timmer, B.J.J., Tai, C.W., Li, X., Xie, Z., Meng, Q., Fan, L., Zhang, F., Ahlquist, M.S.G., Cuartero, M., Crespo, G.A., Sun, L., 2020, Molybdenum and boron synergistically boosting efficient electrochemical nitrogen fixation, Nano Energy, 78, 105391.

Hua, W., Sun, H.H., Xu, F., Wang, J.G., 2020, A review and perspective on molybdenum-based electrocatalysts for hydrogen evolution reaction, Rare Metals, 39, 335-351.

Imam, M., Gaul, K., Stegmüller, A., Höglund, C., Jensen, J., Hultman, L., Birch, J., Tonner, R., Pedersen, H., 2015, Gas phase chemical vapor deposition chemistry of triethylboron probed by boron-carbon thin film deposition and quantum chemical calculations, J Mater Chem C Mater, 3, 10898–10906.

Kou, T., Chen, M., Wu, F., Smart, T.J., Wang, S., Wu, Y., Zhang, Y., Li, S., Lall, S., Zhang, Z., Liu, Y.S., Guo, J., Wang, G., Ping, Y., Li, Y., 2020, Carbon doping switching on the hydrogen adsorption activity of NiO for hydrogen evolution reaction, Nat Commun, 11-590

Kumar, R., Soam, A., Dusane, R.O., Bhargava, P., 2018, Sucrose derived carbon coated silicon nanowires for supercapacitor application, Journal of Materials Science: Materials in Electronics, 29, 1947–1954.

Mazaheri, A., Javadi, M., Abdi, Y., 2021, Chemical vapor deposition of two-dimensional boron sheets by thermal decomposition of diborane, ACS Appl Mater Interfaces, 13, 8844–8850.

Ramji, H.R., Glandut, N., Orlianges, J.-C., Absi, J., Lim, S.F., 2025, Kinetic Study and Simulation of Titanium Carbide-Supported, Platinum-Doped Tetrahedral Amorphous Carbon Electrodes for Hydrogen Evolution Reaction, Materials, 18-1916.

Ramji, H.R., Ibidin, M.Q.Z., Glandut, N., Absi, J., Fong, L.S., 2024, Kinetic study and simulation of molybdenum borides for hydrogen evolution reaction, International Journal of Advances in Applied Sciences, 13, 698–706.

Saini, R., Naaz, F., Bashal, A.H., Pandit, A.H., Farooq, U., 2023, Recent advances in nitrogen-doped graphene-based heterostructures and composites: mechanism and active sites for electrochemical ORR and HER, Green Chemistry, 26, 57-102.

Shinagawa, T., Garcia-Esparza, A.T., Takanabe, K., 2015, Insight on Tafel slopes from a microkinetic analysis of aqueous electrocatalysis for energy conversion, Sci Rep, 5-13801.

Shiva Kumar, S., Himabindu, V., 2020, Boron-Doped Carbon nanoparticles supported palladium as an efficient hydrogen evolution electrode in PEM water electrolysis, Renew Energy, 146, 2281–2290.

Wang, X., Tai, G., Wu, Z., Hu, T., Wang, R., 2017, Ultrathin molybdenum boride films for highly efficient catalysis of the hydrogen evolution reaction, J Mater Chem A Mater, 5, 23471–23475.

Wei, Z.D., Ji, M.B., Chen, S.G., Liu, Y., Sun, C.X., Yin, G.Z., Shen, P.K., Chan, S.H., 2007, Water electrolysis on carbon electrodes enhanced by surfactant, Electrochim Acta, 52, 3323–3329.

Yu, E., Pan, Y., 2024, Enhancing the catalytic hydrogen evolution reaction (HER) of the defective borophene@Pt/Pd/MoS2 heterojunction, Int J Hydrogen Energy, 50, 920–931.